e-J. Surf. Sci. Nanotech. Vol. 13 (2015) 231-234 Conference - ISSS-7 -

# Origin of Repulsive Interactions between Bunched Steps on Vicinal Solid Surfaces*

Keisuke Sawada,† Jun-Ichi Iwata, and Atsushi Oshiyama
*Department of Applied Physics, The University of Tokyo, 7-3-1 Hongo, Tokyo 113-8656, Japan*
(Received 13 January 2015; Accepted 13 May 2015; Published 23 May 2015)

We investigate the origin of repulsive interactions between atomic steps on vicinal solid surfaces using a first-principles approach. Peculiar electronic states localized near step edges are found in $(11\bar{2}n)$ nanofacets formed on the 4H-SiC(0001) vicinal surface. The localized states are gradually overlapped between the steps with shrinking the distance between atomic steps. From a viewpoint of energetics for $(11\bar{2}n)$ nanofacets, the presence of the repulsive interaction between atomic steps is expected. We then suggest that the overlap between electrons distributed around step edges is a possible origin of the step-step repulsive interaction. [DOI: 10.1380/ejssnt.2015.231]

Keywords: Density functional calculations; Faceting; Step formation and bunching; Silicon carbide

## I. INTRODUCTION

Surfaces of crystals show different behaviors from the inside of crystals, such as surface reconstruction and surface relaxation [1, 2]. These phenomena induce novel nanostructures on surfaces. One of such surface nanostructures is the nanofacet which is the unexpected and spontaneous appearance of the small-area surface with the high Miller index on the low Miller index substrate surface. The nanofacet is often formed by step bunching during the epitaxial growth of substrates [3–7]. According to the classical elastic theory [8–10] and phenomenological theory [11–13], the step bunching is caused by the competition between the difference of growth kinetics of each atomic step and repulsive interactions between the steps. The step-step repulsive interaction is an important origin for the emergence of step bunching. Therefore, it is crucial to understand the microscopic details of atomic steps by considering the quantum mechanical effects beyond the elastic theories [10].

The electronic-structure calculations based on the first-principles methods include quantum effects beyond the elastic theory and have been applied successfully to clarify the microscopic details of atomic steps. For example, for the {311} facet observed in the epitaxial growth on the Si(100) surface [7], a density-functional-theory (DFT) calculation has revealed that the anisotropic diffusivity of the Si adatom near the double-layer steps leads to the {311} facet formation [14]. For the $(11\bar{2}n)$ nanofacets formed on the vicinal SiC(0001) surface [15, 16], the DFT calculation has also clarified that a competition between the step-step repulsive interaction and the surface-energy variation, which comes from the different bilayer atomic sequence near the SiC(0001) surface, is the reason for the faceting [17]. Although the step-step repulsive interaction has been discussed for the formation of the $(11\bar{2}n)$ nanofacets, the electronic structures around atomic steps have not been investigated yet.

In this paper, we perform the first-principles electronic-structure calculations on the $(11\bar{2}n)$ nanofacet formed on the vicinal 4H-SiC(0001) surface and clarify a relation between the repulsive interactions and electron states of atomic steps. First, we find localized electron states near the step edges. The energy bands of these states are energetically separated from the energy bands of dangling bonds on terrace surfaces and covalent bonds inside bulk. By comparing the characters of the Kohn-Sham (KS) orbitals of the edge states in the $(11\bar{2}n)$ nanofacets in the range of $n$ from 32 to 4, we exemplify the existence of the step-step repulsive interaction.

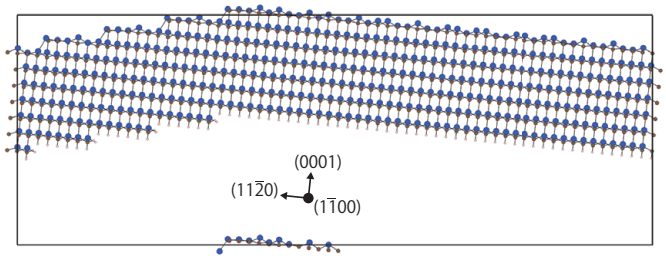


FIG. 1. Side view of the calculational model for the $(11\bar{2}n)$ nanofacet formed on the 4H-SiC(0001) vicinal surface. The large blue, middle brown, and small pink balls denote the Si, C and H atoms, respectively. The rectangle indicates the unit cell and 968 atoms are included. The sequence of the biatomic layers is ABCB from the top most surface at the longest terrace. The $(11\bar{2}n)$ $(n = 12)$ nanofacet with the facet angle $\varphi = 15.3^\circ$ is displayed in this figure.

## II. COMPUTATIONAL METHOD

All calculations are based on the DFT in conjunction with a local density approximation [18]. We have adopted a real-space scheme [19, 20] in the DFT and have developed a highly efficient computation code named RSDFT [21]. The three-dimensional discrete-grid points are introduced in the real space and differential operators for kinetic energy are replaced by finite-difference operators with sufficiently high orders. The RSDFT shows good scalability even with 80,000 compute nodes at K computer at Kobe, Japan [22, 23]. Hence, our real-space scheme is very suitable as large-scale DFT calculations on massively parallel computers [21–23]. The norm-conserving pseudopotential method is employed to describe the ion-electron interactions [24]. The grid spacing in the real space is taken to be 0.22 Å corresponding to a cutoff energy of 57 Ry in the plane-wave-basis-set calculations. We

* This paper was presented at the 7th International Symposium on Surface Science, Shimane Prefectural Convention Center (Kunibiki Messe), Matsue, Japan, November 2-6, 2014.
† Corresponding author: sawada@comas.t.u-tokyo.ac.jp

  

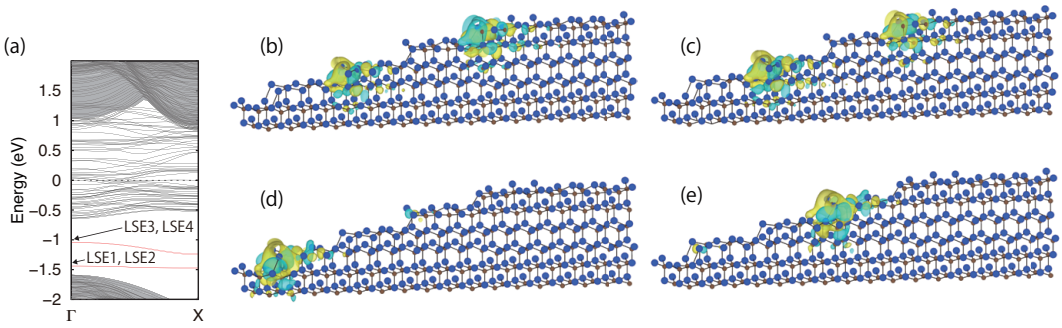


FIG. 2. Electronic structures on the $(11\bar{2}n)$ ($n = 12$) nanofacet with the facet angle $\varphi = 15.3°$ formed on the vicinal 4H-SiC(0001) surface. (a) denotes band dispersions along the Γ-X direction which corresponds to the step-edge direction. The Fermi level is set to zero. The energy bands originated from the localized-step-edge (LSE) states are lying at −1 eV and −1.5 eV (see text). They are marked by red lines and labeled as LSE1, LSE2, LSE3 and LSE4. The energy bands of the 4H-SiC bulk are toned by gray-shaded regions. (b), (c), (d), and (e) depict the Kohn-Sham (KS) orbitals at the Γ point for the LSE1, LSE2, LSE3, and LSE4, respectively. The yellow and light blue isosurfaces correspond to positive and negative values of the KS orbitals, respectively.

consider a periodic nanofacet on the vicinal 4H-SiC(0001) surface with the Si face observed by atomic force microscope and transmission electron microscope [16]. The nanofacet is formed on the surface inclining with the vicinal angle $\theta = 5.9°$ from (0001) basal planes on substrates and faceted with specific facet angle $\varphi$ angles between the $(11\bar{2}n)$ and (0001) directions. In order to simulate the periodic $(11\bar{2}n)$ nanofacets on the vicinal 4H-SiC(0001) surface, we use a repeating slab model tilted by $\theta = 5.9°$ as shown in Fig. 1. The facet angle $\varphi$ is controlled by changing the width of each terrace surface. The each slab consists of seven SiC bilayers and the four single-height-steps consisting of one SiC bilayer are involved in the unit cell. The unit length along the $(1\bar{1}00)$ (parallel to the edge) direction is taken to be 5.27 Å, which is the calculated lattice constant of the crystalline 4H-SiC. Periodic images of the slab model are separated by the vacuum region with the thickness of 10 Å. We sample the 4-$k$ points along the step-edge direction for Brillouin-zone integration. The geometry optimization is carried out until the remaining forces become less than 50 meV/Å. The positions of the bottom SiC bilayer passivated by H atoms are fixed throughout the geometry optimization.

## III. RESULTS AND DISCUSSION

We first investigate the electronic structure on the $(11\bar{2}n)$ ($n = 12$) nanofacet with the facet angle $\varphi = 15.3°$ formed on the 4H-SiC(0001) vicinal surface. The nanofacet with the angle $\varphi = 15.3°$ is the most stable among those with several different angles [17] and $\varphi = 15.3°$ is close to experimentally observed facet angle $\varphi_{\mathrm{Expt.}} = 12°$ [16]. Figure 2 (a) shows the electronic band structure on the $(11\bar{2}n)$ ($n = 12$) nanofacet. We find dispersion-less isolated and doubly degenerated bands at −1 eV and −1.5 eV. Figure 2 (b)-(e) describe the characters of the KS orbitals at the Γ point for the isolated bands. Interestingly, we find that the KS orbitals are spatially localized around the step edges in the $(11\bar{2}n)$ ($n = 12$) nanofacet. Hereafter, these localized states are referred to as the localized-step-edge (LSE) states.

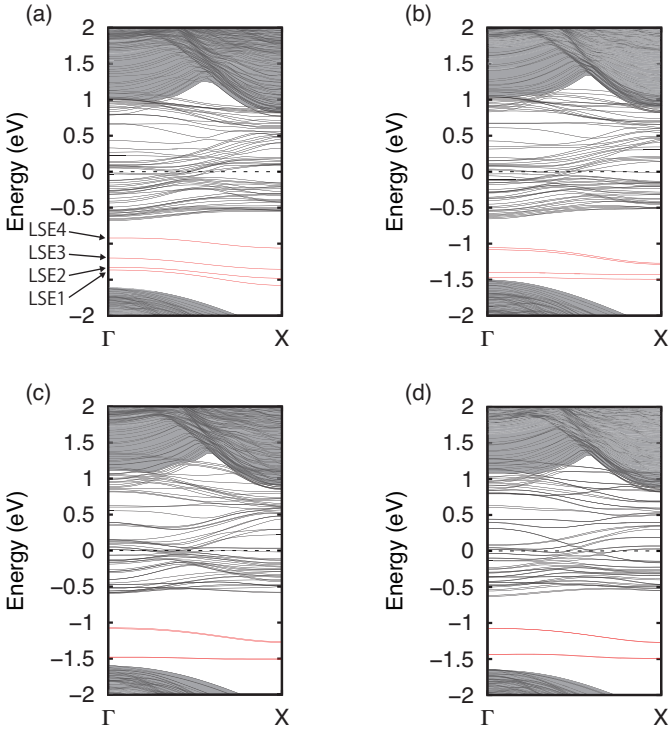


FIG. 3. Electronic band structures on the $(11\bar{2}n)$ ($n = 4$) (a), ($n = 8$) (b), ($n = 24$) (c), and ($n = 32$) (d) nanofacets formed on the vicinal 4H-SiC(0001) surface. The facet angles of these nanofacets are $\varphi = 39.2$, 22.3, 7.8, and 5.9°, respectively. The Fermi level is set to zero. The energy bands originated from the LSE states are marked by red lines. In (a), they are labeled as LSE1, LSE2, LSE3 and LSE4. The energy bands of the 4H-SiC bulk are toned by gray-shaded regions.

We also find that many energy bands near the $E_{\mathrm{F}}$ are the states of dangling bonds on terraces at the $(11\bar{2}n)$ ($n = 12$) nanofacet, and valence bands of the 4H-SiC bulk are located at more than 1.5 eV below the $E_{\mathrm{F}}$.

Next, we explore a behavior of the electronic structures of $(11\bar{2}n)$ nanofacets in terms of the distance between the steps. Since the distance between atomic steps can be

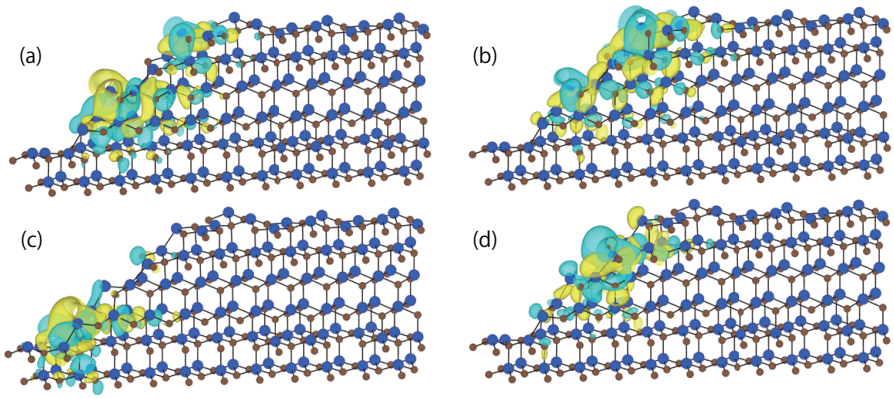


FIG. 4. Kohn-Sham (KS) orbitals on the $(11\bar{2}n)$ $(n = 4)$ nanofacet with the facet angle $\varphi = 39.2°$ formed on the vicinal 4H-SiC(0001) surface. (a), (b), (c), and (d) describe the KS orbitals at the Γ point for the LSE1, LSE2, LSE3, and LSE4 as marked in Fig. 3 (a), respectively. The yellow and light blue isosurfaces correspond to positive and negative values of the KS orbitals, respectively.

adjusted by varying $\varphi$ in the $(11\bar{2}n)$ nanofacet, we compare the electronic band structures of $(11\bar{2}n)$ nanofacets with several facet angles. Figure 3 shows the electronic band structures on $(11\bar{2}n)$ nanofacets with several facet angles. We find that four energy bands coming from the LSE states do not degenerate in the $(11\bar{2}n)$ $(n = 4)$ and $(n = 8)$ nanofacets with $\varphi = 39.2$ and 22.3°, respectively whereas they degenerate in the $(11\bar{2}n)$ $(n = 12)$, $(n = 24)$, and $(n = 32)$ nanofacets with $\varphi = 15.3$, 7.8 and 5.9°, respectively. Moreover, we notice that the band degeneracies begin to occur in the facet angle smaller than $\varphi = 15.3°$ which corresponds to the most stable nanofacet.

Our first-principles study previously predicted that the $(11\bar{2}n)$ $(n = 4)$ and $(n = 8)$ nanofacets with $\varphi = 39.2$ and 22.3° were energetically much unstable than the $(11\bar{2}n)$ $(n = 12)$, $(n = 24)$, and $(n = 32)$ nanofacets with $\varphi = 15.3$, 7.8, and 5.9° [17]. Our previous study also showed that the $(11\bar{2}n)$ $(n = 4)$ nanofacet with $\varphi = 39.2°$ has the longest terrace with the ABC stacking sequence from the top most surface, and the surface with this stacking sequence is more stable than that with other stacking sequences. Nevertheless, the $(11\bar{2}n)$ $(n = 4)$ and $(n = 8)$ nanofacets with relatively short step-step distance are higher in energy than the $(11\bar{2}n)$ $(n = 12)$, $(n = 24)$, and $(n = 32)$ nanofacets with relatively long step-step distance.

According to the elastic theory [10], the step-step repulsive interaction decreases with increasing the distance between atomic steps and quadratically decays in the long-enough step-step distance. Therefore, this suggests that there is a step-step repulsive interaction which overwhelms the stability of long ABC-stacking terraces of the nanofacets with $\varphi > 15.3°$.

In order to elucidate the reason for the splitting of energy bands of the LSE states and the instabilities in energetics in the region of $\varphi > 15.3°$, we depict the characters of the KS orbitals in the $(11\bar{2}n)$ $(n = 4)$ nanofacet with $\varphi = 39.2°$. Figure 4 denotes the characters of the KS orbitals at the Γ point for the LSE1, LSE2, LSE3, and LSE4 as indicated in Fig. 3 (a). We find that the LSE states overlap with each other and this causes the splitting of energy bands of the LSE states. In contrast, the KS orbitals of the LSE states at the $(11\bar{2}n)$ $(n = 12)$ nanofacet with $\varphi = 15.3°$ don't overlap with each other and the atomic structure of each terrace near the step is the same, and in this case the energy bands degenerate as shown in Fig. 2.

Based on the above results, we can deduce that the overlap of the KS orbitals affects the stability of the $(11\bar{2}n)$ nanofacet. In other words, the electronic localization near step edges implies that the step-step repulsive interaction becomes negligibly small. Consequently, we argue that the overlap between wavefunctions distributed around each step edges is a possible origin of the step-step repulsive interaction.

## IV. SUMMARY

We performed first-principles electronic-structure calculations on the $(11\bar{2}n)$ nanofacets with several facet angles formed on the vicinal 4H-SiC(0001) surface. In the $(11\bar{2}n)$ nanofacets in the range of $\varphi \leq 15.3°$, we found peculiar electronic states localized around the step edges and four energy bands originated from the localized-step-edge states. We also found that these bands degenerated in the regions of $\varphi \leq 15.3°$ and split in $\varphi > 15.3°$. The existence of the step-step repulsive interaction was implicated by investigating the relation between the energetics and surface stability in the $(11\bar{2}n)$ nanofacet. For $(11\bar{2}n)$ nanofacets in the range of $\varphi > 15.3°$ with substantially short step-step distance, we clarified that the splitting of these bands was caused by overlaps between wavefunctions located near each step edge. Therefore, we suggested that these overlaps are a possible origin of the repulsive interaction between steps in $(11\bar{2}n)$ nanofacets. These findings and analyses greatly contribute to evolutions of fundamental physics for surface science and surface nanotechnology.

## ACKNOWLEDGMENTS

This work was supported by the Grants-in-Aid for scientific research under Contract No. 22104005 and also by "Computational Materials Science Initiative", both conducted by MEXT, Japan. Computations were performed

mainly at K Computer in Advanced Institute for Computational Science, RIKEN.

[1] P. M. Petroff, A. Lorke, and A. Imamoglu, Phys. Today **54**, 46 (2001).
[2] J. Stangl, V. Holý, and G. Bauer, Rev. Mod. Phys. **76**, 725 (2004).
[3] A. Shchukin and D. Bimberg, Rev. Mod. Phys. **71**, 1125 (1999).
[4] S. Rousset, F. Pourmir, J. M. Berroir, J. Klein, J. Lecoeur, P. Hecquet, and B. Salanon, Surf. Sci. **422**, 33 (1999).
[5] M. Giesen and T. L. Einstein, Surf. Sci. **449**, 191 (2000).
[6] D. J. Eaglesham, F. C. Unterwald, and D. C. Jacobson, Phys. Rev. Lett. **70**, 966 (1993).
[7] H. Hirayama, M. Hiroi, and T. Ide, Phys. Rev. B **48**, 17331 (1993).
[8] O. L. Alerhand, D. Vanderbilt, R. D. Meade, and J. D. Joannopoulos, Phys. Rev. Lett. **61**, 1973 (1988).
[9] O. L. Alerhand, A. N. Berker, J. D. Joannopoulos , D. Vanderbilt, R. J. Hamers, and J. E. Demuth, Phys. Rev. Lett. **64**, 2406 (1990).
[10] V. I. Marchenko and A. Y. Parshin, Zh. Eksp. Teor. Fiz. **79**, 256 (1980) [JETP **52**, 129 (1980)].
[11] R. L. Schwoebel and E. E. J. Shipsey, J. Appl. Phys. **37**, 3682 (1966).
[12] M. Sato and M. Uwaha, Phys. Rev. B **51**, 11172 (1995).
[13] H. C. Jeong and E. D. Williams, Surf. Sci. Rep. **34**, 171 (1999).
[14] A. Oshiyama, Phys. Rev. Lett. **74**, 130 (1995).
[15] H. Nakagawa, S. Tanaka, and I. Suemune, Phys. Rev. Lett. **91**, 226107 (2003).
[16] M. Fujii and S. Tanaka, Phys. Rev. Lett. **99**, 016102 (2007).
[17] K. Sawada, J.-I. Iwata, and A. Oshiyama, Appl. Phys. Lett. **104**, 051605 (2014).
[18] J. P. Perdew and A. Zunger, Phys. Rev. B **23**, 5048 (1981).
[19] J. R. Chelikowsky, N. Troullier, and Y. Saad, Phys. Rev. Lett. **72**, 1240 (1994).
[20] J.-I. Iwata, K. Shiraishi, and A. Oshiyama, Phys. Rev. B **77**, 115208 (2008).
[21] J.-I. Iwata, D. Takahashi, A. Oshiyama, B. Boku, K. Shiraishi, S. Okada, and K. Yabana, J. Comput. Phys. **229**, 2339 (2010).
[22] Y. Hasegawa, J.-I. Iwata, M. Tsuji, D. Takahashi, A. Oshiyama, K. Minami, T. Boku, F. Shoji, A. Uno, M. Kurokawa, H. Inoue, I. Miyoshi, and M. Yokokawa, Proceedings of 2011 International Conference for High Performance Computing, Networking, Storage and Analysis (SC2011, Seatle, USA) artcle no 1, doi: 10.1145/2063384.2063386
[23] Y. Hasegawa, J.-I. Iwata, M. Tsuji, D. Takahashi, A. Oshiyama, K. Minami, T. Boku, H. Inoue, Y. Kitazawa, I. Miyoshi, and M. Yokokawa, Int. J. HPC Applications (2013) (published online), doi: 10.1177/1094342013508163
[24] N. Troullier and J. L. Martins, Phys. Rev. B **43**, 1993 (1991).